BMJ Open Diabetes Research & Care

AI-enabled opportunistic measurement of liver steatosis in coronary artery calcium scans predicts cardiovascular events and all-cause mortality: an AI-CVD study within the Multi-Ethnic Study of Atherosclerosis (MESA)

Morteza Naghavi ,[1] Kyle Atlas,[1] Anthony Reeves,[2] Chenyu Zhang,[1] Jakob Wasserthal,[3] Thomas Atlas,[4] Claudia I. Henschke,[5] David F. Yankelevitz,[5] Javier J Zulueta,[5] Matthew J Budoff,[6] Andrea D Branch,[5] Ning Ma,[7] Rowena Yip,[5] Wenjun Fan,[8] Sion K Roy,[6] Khurram Nasir,[9] Sabee Molloi,[8] Zahi Fayad,[7] Michael V McConnell,[10] Ioannis Kakadiaris,[11] David J Maron,[10] Jagat Narula,[12] Kim Williams,[13] Prediman K Shah,[14] George Abela,[15] Rozemarijn Vliegenthart,[16] Daniel Levy,[17] Nathan D. Wong[8]

To cite: Naghavi M, Atlas K, Reeves A, *et al*. AI-enabled opportunistic measurement of liver steatosis in coronary artery calcium scans predicts cardiovascular events and all-cause mortality: an AI-CVD study within the Multi-Ethnic Study of Atherosclerosis (MESA). *BMJ Open Diab Res Care* 2025;**13**:e004760. doi:10.1136/bmjdrc-2024-004760

► Additional supplemental material is published online only. To view, please visit the journal online (https://doi.org/10.1136/bmjdrc-2024-004760).

Received 15 November 2024
Accepted 6 March 2025

For numbered affiliations see end of article.

Correspondence to
Dr Morteza Naghavi;
mn@vp.org

ABSTRACT

Introduction About one-third of adults in the USA have some grade of hepatic steatosis. Coronary artery calcium (CAC) scans contain more information than currently reported. We previously reported new artificial intelligence (AI) algorithms applied to CAC scans for opportunistic measurement of bone mineral density, cardiac chamber volumes, left ventricular mass, and other imaging biomarkers collectively referred to as AI-cardiovascular disease (CVD). In this study, we investigate a new AI-CVD algorithm for opportunistic measurement of liver steatosis.

Methods We applied AI-CVD to CAC scans from 5702 asymptomatic individuals (52% female, age 62±10 years) in the Multi-Ethnic Study of Atherosclerosis. Liver attenuation index (LAI) was measured using the percentage of voxels below 40 Hounsfield units. We used Cox proportional hazards regression to examine the association of LAI with incident CVD and mortality over 15 years, adjusted for CVD risk factors and the Agatston CAC score.

Results A total of 751 CVD and 1343 deaths accrued over 15 years. Mean±SD LAI in females and males was 38±15% and 43±13%, respectively. Participants in the highest versus lowest quartile of LAI had greater incidence of CVD over 15 years: 19% (95% CI 17% to 22%) vs 12% (10% to 14%), respectively, p<0.0001. Individuals in the highest quartile of LAI (Q4) had a higher risk of CVD (HR 1.43, 95% CI 1.08 to 1.89), stroke (HR 1.77, 95% CI 1.09 to 2.88), and all-cause mortality (HR 1.36, 95% CI 1.10 to 1.67) compared with those in the lowest quartile (Q1), independent of CVD risk factors.

Conclusion AI-enabled liver steatosis measurement in CAC scans provides opportunistic and actionable information for early detection of individuals at elevated risk of CVD events and mortality, without additional radiation.

WHAT IS ALREADY KNOWN ON THIS TOPIC

⇒ Liver steatosis is a marker of metabolic dysfunction and cannot be directly diagnosed using blood tests; however, a variety of imaging modalities are available for non-invasive detection.

WHAT THIS STUDY ADDS

⇒ Artificial intelligence (AI)-enabled CT attenuation analysis of the liver in new or existing coronary artery calcium scans is feasible and provides opportunistic and actionable information for early detection of patients at elevated risk of cardiovascular disease.

HOW THIS STUDY MIGHT AFFECT RESEARCH, PRACTICE OR POLICY

⇒ This study demonstrates that AI-enabled CT attenuation analysis of the liver offers a rapid, cost-effective, and scalable approach for opportunistically detecting hepatic steatosis, enabling broader cardiovascular risk assessment in populations not typically evaluated for this subclinical condition

INTRODUCTION

About one-third of adults in the USA have some degree of fatty liver, or hepatic steatosis, a condition in which hepatocytes have an excessive accumulation of fat, mainly in the form of triglycerides.[1] The two most common forms of fatty liver diseases are non-alcoholic fatty liver disease (NAFLD) and alcohol-associated liver disease (ALD), but NAFLD is the more prevalent form in high-income

countries, often associated with obesity, insulin resistance, and metabolic syndrome. Recently, the term metabolic dysfunction associated steatotic liver disease (MASLD) was introduced to emphasize the importance of metabolic dysfunction in NAFLD. MASLD is by far the most prevalent chronic liver disease globally.[2] ALD is less prevalent,[3] but associated with higher mortality. The case definition of MASLD requires liver steatosis and at least one of five cardiometabolic risk factors (obesity, prediabetes/diabetes, hypertension, high triglycerides, low high-density lipoprotein (HDL).[4] The intertwining of MASLD, cardiovascular-kidney-metabolic health, and cardiometabolic risk factors is a complex interaction that raises the question of whether steatotic liver disease is itself an independent predictor of cardiovascular disease (CVD).[5 6] This is an especially compelling area of investigation because the liver is the metabolic hub of the body and the processing site of triglycerides and lipoprotein particles—blood constituents that are well-known drivers of cardiovascular risk.

Liver steatosis cannot be directly diagnosed using blood tests; however, a variety of imaging modalities are available for non-invasive detection.[7] Although liver biopsy and MRI provide the most sensitive and accurate quantitation of liver fat,[7] they are not suitable as an opportunistic screening tool for quantification of liver fat. Similarly, liver ultrasound elastography, although more commonly available and less precise, is not suitable as an opportunistic screening test. Non-contrast CT scans of the chest or abdomen provide for opportunistic detection of moderate-to-severe steatosis. Every year, >80 million abdominal and thoracic CT scans are performed in the USA alone,[8] including CT scans for coronary artery calcium (CAC) scoring and lung cancer screening, which can be used for opportunistic detection of liver steatosis. The resulting scans provide valuable data, which can be extracted and used to detect moderate-to-severe steatosis at no additional X-ray or imaging cost to the patient and enable providers to gain important information. In CT imaging, liver attenuation measured in Hounsfield units (HU) is inversely related to liver fat content, with lower HU values indicating higher fat content.[9] In particular, a mean density <40 HU is correlated with at least 30% steatosis (moderate-to-severe) on histopathology.[10 11] This method provides a reliable, reproducible indication of moderate-to-severe steatosis, making it a valuable tool in both clinical and research settings for evaluating metabolic health and its associated risks.[12 13]

AI-CVD is a suite of AI software modules that enables opportunistic screening for multiple disorders in chest CT scans including non-contrast CAC, contrast-enhanced coronary CT angiography (CCTA), and low-dose lung cancer screening scans.[14] We have previously published multiple studies on other outputs of AI-CVD from CAC scans in the Multi-Ethnic Study of Atherosclerosis (MESA), including bone mineral density, cardiac chambers volumetry, and left ventricular mass.[15–20] In this study, we applied AI-CVD algorithms to measure hepatic steatosis in MESA CAC scans. Unlike previous CT-based AI-enabled evaluation of liver fat in which only a few spots of the liver are analyzed,[7] our AI algorithms analyze the entire liver in the field of view.

In this paper, we introduce and validate a novel metric, the liver attenuation index (LAI), which reports the percentage of voxels with attenuation below 40 HU (LAI) in non-contrast CAC scans. We evaluate the prognostic value of LAI for incident CVD events and all-cause mortality over 15 years in MESA. Additionally, we correlate LAI with the US fatty liver index (US-FLI), a composite score designed for use in the USA for all races/ethnicities, for indication of steatosis.

METHODS

Study population

MESA is a prospective cohort study that began in July 2000 to investigate the prevalence, correlates, and progression of subclinical CVD in individuals without known CVD at baseline. The cohort included 6814 women and men aged 45–84 years recruited from six US communities (Baltimore, Maryland; Chicago, Illinois; Forsyth County, North Carolina; Los Angeles County, California; Northern Manhattan, New York; and St. Paul, Minnesota). Race/Ethnicity makeup included non-Hispanic White (38%), non-Hispanic Black (28%), Chinese (11%), and Hispanic (11%). Individuals with a history of physician-diagnosed myocardial infarction (MI), angina, heart failure, stroke, or transient ischemic attack, or who had undergone an invasive procedure for CVD (coronary artery bypass graft, angioplasty, valve replacement, pacemaker placement, or other vascular surgeries) were excluded. A detailed study design for MESA has been published elsewhere.[21] For this study, 771 participants who did not consent to commercial use of their data were excluded. Additionally, we removed 340 participants with missing slices in CAC scans, missing outcome data, or missing risk factor data, leaving 5702 CAC scans processed for analysis.

Evaluation of cardiovascular disease and all-cause mortality

Participants were contacted by the MESA research team by telephone every 9–12 months during follow-up and asked to report all new cardiovascular diagnoses. International Classification of Disease (ICD) codes were obtained. The average participant surveillance time was 12.4±3.8 years. Incident CVD for this study is defined as MI, resuscitated cardiac arrest, definite angina, probable angina (if followed by revascularization), non-fatal stroke, fatal stroke, coronary heart disease (CHD) death, other atherosclerotic death, and other CVD-related death. Incident CHD was defined as MI, resuscitated cardiac arrest, angina, and CHD deaths. MI events during exam 1 were ascertained through a combination of self-reports, medical record review, and adjudication by a centralized committee. The MESA Events Committee adjudicated the events by using standard criteria based on symptoms, electrocardiographic changes, cardiac biomarkers, and

imaging findings to confirm the occurrence of MI. Incident stroke was classified as hemorrhagic or ischemic. Stroke was identified as present if there was rapid onset of a documented focal neurological deficit lasting 24 hours or until death, or if <24 hours, there was a clinically relevant lesion on brain imaging. Patients with focal neurological deficits secondary to brain trauma, tumor, infection, or other non-vascular causes were excluded. Transient ischemic attack was not included in this definition.

All-cause mortality in MESA was determined based on annual National Death Index (NDI) searches to identify or confirm participant deaths and included CVD and non-CVD-related deaths. Participants are included in the NDI search if they met any of the following criteria: (a) latest follow-up participant status coded as 'reported deceased', (b) latest follow-up participant status coded as 'unknown,' (c) death has already been investigated, but no death certificate was obtained. If a participant is submitted in an NDI search but is not identified as deceased, they are credited follow-up time.

The AI software for automated liver attenuation

The AI software used for automated liver attenuation quantification in this manuscript is a component of AI-CVD (HeartLung.AI, Houston, Texas, USA), a deep learning model that quantifies numerous anatomical structures in non-contrast or contrast-enhanced cardiac and lung CT images. The region of interest the AI uses for liver attenuation is across the entire liver in the available field of view. Examples of normal liver and severely steatotic liver are shown in figure 1.

The core machine learning component of AI-CVD is adapted from TotalSegmentator, which is a widely used anatomical model published and validated by investigators independent from our group.[22] The source code for the base architecture of TotalSegmentator is available publicly from GitHub.[23] The TotalSegmentator model was trained and validated on 1139 whole-body CT examinations cases with 447 cases of CCTA randomly sampled from the University Hospital Basel picture archiving and communication system. The model used a nnU-Net, a self-configuring method for deep learning-based biomedical image segmentation. MESA CT examinations were not chosen due to lack of contrast-enhanced cardiac CT scans, which are required for nnU-Net training. Furthermore, training on MESA would have resulted in overfitting. The initial input training data were paired non-contrast and ECG-gated cardiac CT scans of the same individuals with 1.5 mm slice thickness. Because the images were taken from identical sessions, registration was accomplished with good alignment. Following this transfer of segmentations, a nnU-Net deep learning tool was used for training the model. Quality control was implemented to detect and count the number of dropped slices in the CT scan. Additionally, cases with no liver available in the field of view were removed from analysis (n=274).

To improve the model for liver fat quantification, we evaluated multiple voxel intensity thresholds to identify the optimal range of HU values for liver fat estimation. The range was determined based on its correlation with established risk factors for hepatic steatosis, its predictive accuracy for relevant clinical outcomes, and its consistency with known HU values of liver tissue and macrovacuolar hepatocytes. The final range of (−30, 70) HU was chosen to maximize the reliability of these associations for calculating the percentage of liver attenuation <40 HU (LAI). Additionally, we have analyzed and are reporting here the mean HU in the AI-segmented liver or part thereof, within the Z range of the CT scan.

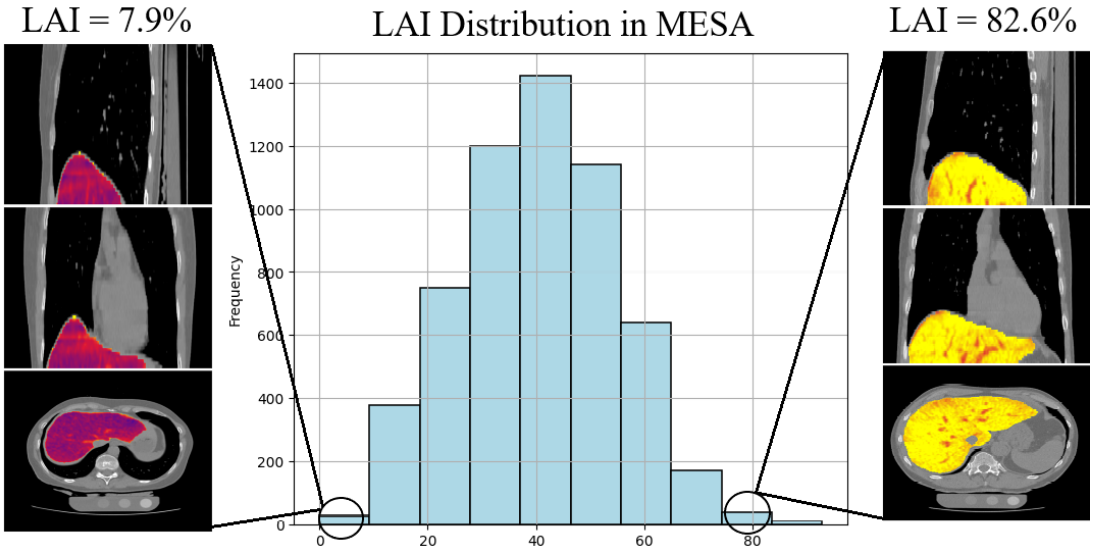

Figure 1 Examples of artificial intelligence-cardiovascular disease liver segmentations in a typical coronary artery calcium (CAC) scan along with the distribution of liver attenuation index (LAI) in Multi-Ethnic Study of Atherosclerosis (MESA)-1.

Table 1 Baseline characteristics of MESA-1 participants overall and by quartiles of LAI

	Overall	First quartile LAI (<32%)	Second quartile LAI (32%–41%)	Third quartile LAI (41%–48%)	Fourth quartile LAI (>48%)
Age (years)	61.76±10.24	61.27±10.59	61.77±10.45	62.6±10.10	61.25±9.85
Sex (female)	46.30%	62.70%	47.80%	40.10%	35.10%
White (%)	45.30%	53.6%	43.50%	41.80%	40.40%
Chinese (%)	7.10%	9.00%	9.10%	6.90%	3.90%
Black (%)	27.00%	28.00%	27.00%	27.20%	26.60%
Hispanic (%)	20.70%	9.40%	20.40%	24.10%	29.10%
Body mass index (kg/m^2)	28.44±5.37	25.0±3.82	27.11±4.17	29.13±4.41	32.66±5.65
Waist circumference (cm)	98.67±14.23	88.72±11.24	95.09±11.33	100.87±11.27	110.33±13.4
LDL cholesterol (mg/dL)	117.01±31.17	115.89±30.89	119.03±31.47	117.55±30.3	115.66±31.14
HDL cholesterol (mg/dL)	51.14±15.17	56.44±15.79	52.71±15.74	49.79±14.25	45.28±12.28
Total cholesterol (mg/dL)	193.21±34.48	193.71±33.75	195.22±34.53	193.36±33.64	190.41±34.78
Systolic blood pressure (mm Hg)	125.5±20.95	122.81±21.89	124.93±21.39	126.94±20.18	127.75±19.86
Diastolic blood pressure (mm Hg)	72.0±10.18	70.0±10.11	71.89±10.43	73.12±9.58	73.31±10.35
Glucose (mg/dL)*	90.00 (83.0, 99.0)	85.00 (80.0, 92.0)	89.00 (82.0, 96.0)	91.00 (84.0, 100.0)	95.00 (87.0, 110.0)
US-fatty liver index*	1.27 (0.55, 2.97)	0.55 (0.27, 1.05)	0.99 (0.49, 1.9)	1.55 (0.79, 3.14)	3.41 (1.72, 6.77)
Pack years of smoking*	2.10 (0.0, 19.5)	1.00 (0.0, 18.0)	2.80 (0.0, 18.5)	2.25 (0.0, 20.5)	2.50 (0.0, 20.42)
Triglycerides (mg/dL)	125.29±65.77	106.9±55.01	117.4±61.5	130.13±66.65	147.33±71.38
C reactive protein (mg/L)*	1.88 (0.83, 4.16)	1.27 (0.59, 3.12)	1.52 (0.74, 3.66)	1.97 (0.93, 4.23)	2.92 (1.34, 5.68)
Interleukin-6 (pg/mL)	1.57±1.25	1.31±1.23	1.39±1.09	1.65±1.22	1.93±1.34
Insulin (mU/L)*	8.02 (5.9, 11.76)	6.27 (4.9, 8.27)	7.27 (5.65, 10.27)	8.64 (6.4, 12.14)	11.76 (8.4, 16.61)
Alcoholic drinks per week*	2.00 (0.0, 6.0)	1.00 (0.0, 5.0)	2.00 (0.0, 6.0)	2.00 (0.0, 6.0)	2.00 (0.0, 7.0)
Diabetes (yes/no)	11.40%	4.50%	9.00%	11.20%	21.10%
Current smoking (vs former/never)	14.40%	14.80%	15.90%	14.30%	12.70%
Any alcohol usage (past 30 days)	70.30%	69.10%	71.50%	70.40%	69.90%
Hypertension Rx	36.00%	27.40%	32.20%	39.90%	45.30%
Lipid--lowering Rx	16.40%	14.30%	16.20%	17.80%	17.40%

*Highly skewed continuous variables presented using median (IQR).
HDL, high-density lipoprotein; LAI, liver attenuation index; LDL, low-density lipoprotein; MESA, Multi-Ethnic Study of Atherosclerosis; Rx, prescription.

CT scan acquisition

In MESA, baseline cardiac CT scans were obtained using either electron-beam CT (EBCT) (50% R-R) or multidetector CT (MDCT) (80% R-R) based on the field center at which they were scanned. Approximately half of the participants were scanned using EBCT (New York, Illinois, and California sites), and the other half MDCT (MD, MN, and NC sites). Participants were scanned twice within several minutes of each other to reduce interscan variability for CAC scoring. Detailed protocols for CAC scoring have been previously published by MESA investigators.[24]

US-fatty liver index

The US-FLI was developed in the multi-ethnic US National Health and Nutrition

Examination Survey to estimate the likelihood of hepatic steatosis.[25] The index is a non-invasive, algorithm-based score calculated from demographic and clinical variables, including age, body mass index (BMI), waist circumference, triglycerides, and gamma-glutamyl transferase. The US-FLI ranges from 0 to 100, with higher scores indicating a greater probability of fatty liver disease.

Statistical analysis

We used SAS (SAS Institute, Cary, North Carolina, USA) and Python V.3.11 software for statistical analyses. All tests of significance were two-tailed, and significance was defined at type I error (α)=0.05 and type II error (β)=0.20. All analyses met the appropriate sample size and power considerations. Instances where these requirements were not met have been excluded and noted. One-way analysis of variance (ANOVA) was used to calculate significant differences between more than two groups. LAI demonstrated a normal distribution in this cohort. US-FLI was right skewed and log-transformed for correlation analysis. Spearman's correlation coefficient was used

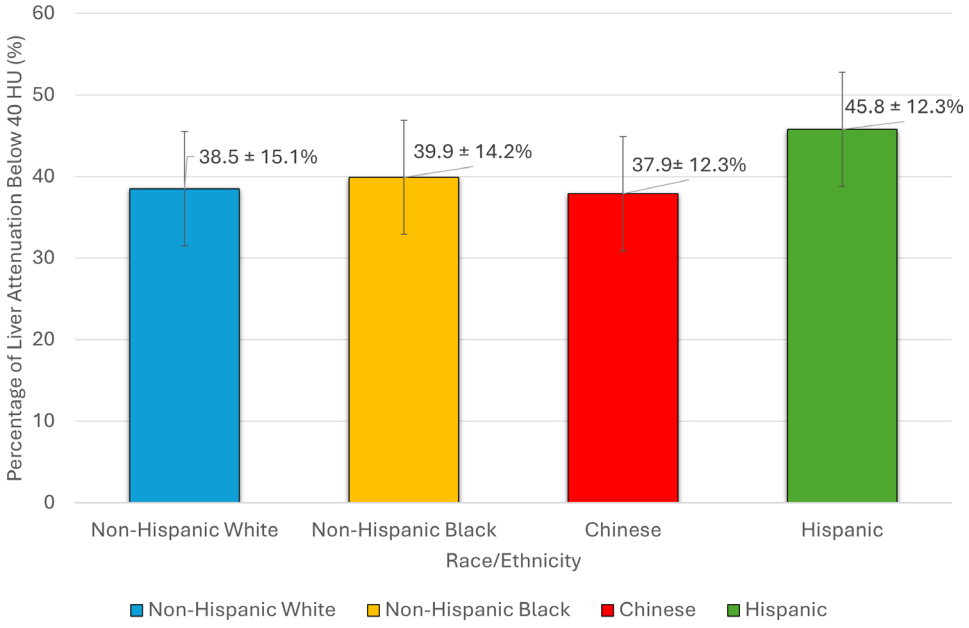

Figure 2 Liver attenuation index by race/ethnicity. HU, Hounsfield units.

to measure the association between LAI and CVD risk factors.

The Cox proportional hazards model was used to assess the association between LAI and incident CVD and mortality. Model assumptions were formally tested using Schoenfeld and Martingale residuals, and no violations of proportional hazards or non-linearity were detected for LAI. HRs are presented per SD increase with 95% CIs and by the top quartile versus the lowest serving as reference. These analyses were minimally adjusted by BMI and fully adjusted for known CVD risk factors: age, dyslipidemia, hypertension, smoking, diabetes, BMI, inflammatory markers such as interleukin-6 (IL-6), insulin, and C reactive protein, and Agatston CAC score. Subgroup analyses of HRs by sex (male/female) and race/ethnicity (non-Hispanic White, Chinese, non-Hispanic Black, Hispanic) were also calculated. The cumulative incidence for CVD events stratified by quartiles of LAI was calculated using one minus the Kaplan-Meier survival estimate. Additionally, we have calculated the cumulative incidence of all CVD among those who fall in the top quartile of CAC score versus LAI versus both. Group differences were determined using the log-rank test.

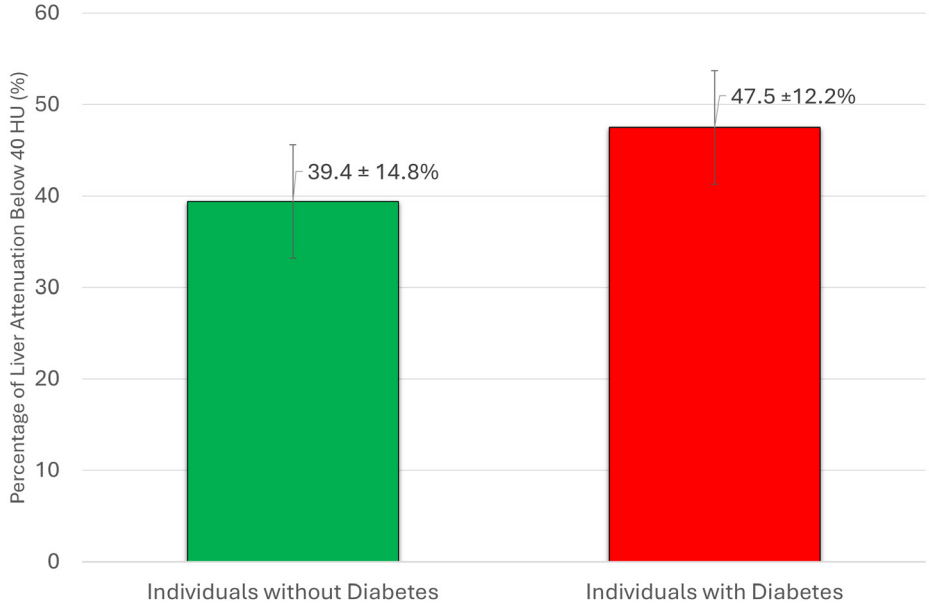

Figure 3 Liver attenuation index in individuals with diabetes versus without diabetes at baseline examination. HU, Hounsfield units.

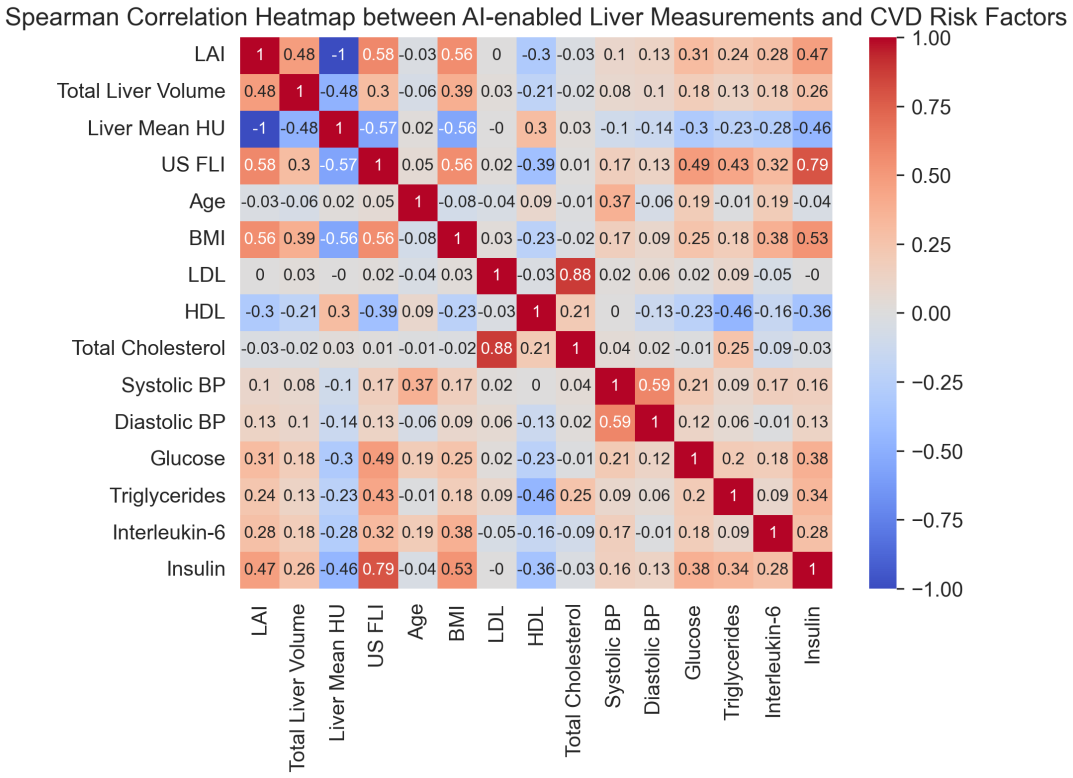

Figure 4 Spearman's correlation between artificial intelligence-cardiovascular disease (AI-CVD) liver measurements and CVD risk factors. BMI, body mass index; BP, blood pressure; HDL, high-density lipoprotein; HU, Hounsfield units; LAI, liver attenuation index; LDL, low-density lipoprotein.

RESULTS

Baseline characteristics and liver-related measurements by quartiles of the study group are presented in table 1. Higher quartiles of LAI were more often male and of higher BMI. Current alcohol usage and drinks per week were consistent across quartiles of LAI, except the lowest quartile, which had one alcoholic drink per week, compared with two drinks per week for the remaining quartiles. An average of 221.7±164.9 cubic centimeters (CC) of liver was analyzed in our study. On average, males had higher liver volume in the scanned image, higher LAI, and higher US-FLI scores than females (p<0.0001). Hispanic participants had higher LAI scores than non-Hispanic White, Chinese, and non-Hispanic Black participants (p<0.001) (figure 2). In univariate analysis, cases with incident CVD events had higher LAI scores than those who did not (42.5% (95% CI 41.7% to 43.4%) vs 40% (39.8% to 40.5%), respectively, p<0.0001). These differences remained statistically significant after adjustment for BMI (p<0.0001) and all CVD risk factors (p=0.03). Additionally, individuals with type 2 diabetes at baseline had higher LAI scores than those without (47.5% vs 39.4%, p<0.0001) (figure 3).

LAI scores had moderate correlation with log-transformed US FLI scores (R=0.57, p<0.0001) (figure 4). Among CVD risk factors, LAI scores had moderate correlation with BMI (R=0.56, p<0.0001) and insulin (R=0.47, p<0.0001), and weak correlation with HDL (r=−0.30, p<0.0001), glucose (R=0.31, p<0.0001), triglycerides (R=0.24, p<0.0001), and IL-6 (R=0.28, p<0.0001. Little correlation was seen with age (R=−0.03, p=0.0128).

Over a mean follow-up of 12.4 years, 751 total CVD events occurred (1.1 per 100 person-years), including 499 CHD events (0.7 per 100 person-years), 236 stroke events (0.3 per 100 person-years), and 1343 all-cause mortality events (1.9 per 100 person-years). Of these, 457 (60.9%) CVD events occurred in males and 294 (39.1%) in females, 330 (66.1%) CHD events occurred in males and 169 (33.9%) in females, 122 (51.7%) stroke events occurred in males and 112 (48.3%) in females, and 747 (55.6%) mortality events in males and 596 (44.4%) mortality events in females. Participants in the highest LAI quartile (>50%) had significantly higher incident CVD over 15 years than those in the lowest quartile (<30%): 19.2% (95% CI 17.1% to 21.5%) vs 11.7% (9.5% to 14.3%), respectively, p<0.0001 (figure 5a). These differences remained even after adjustment for BMI (figure 5b) and diabetes (figure 5c). Participants in the highest quartile of both LAI and CAC score (n=386) experienced 37.3% (32.3% to 42.7%) incidence of all CVD over 15 years (figure 6).

Analysis of quartile-based HRs

In fully adjusted models, individuals in the highest quartile of LAI (Q4) had higher risks of CVD (HR 1.43, 95% CI 1.08 to 1.89), stroke (HR 1.77, 95% CI 1.09 to 2.88),

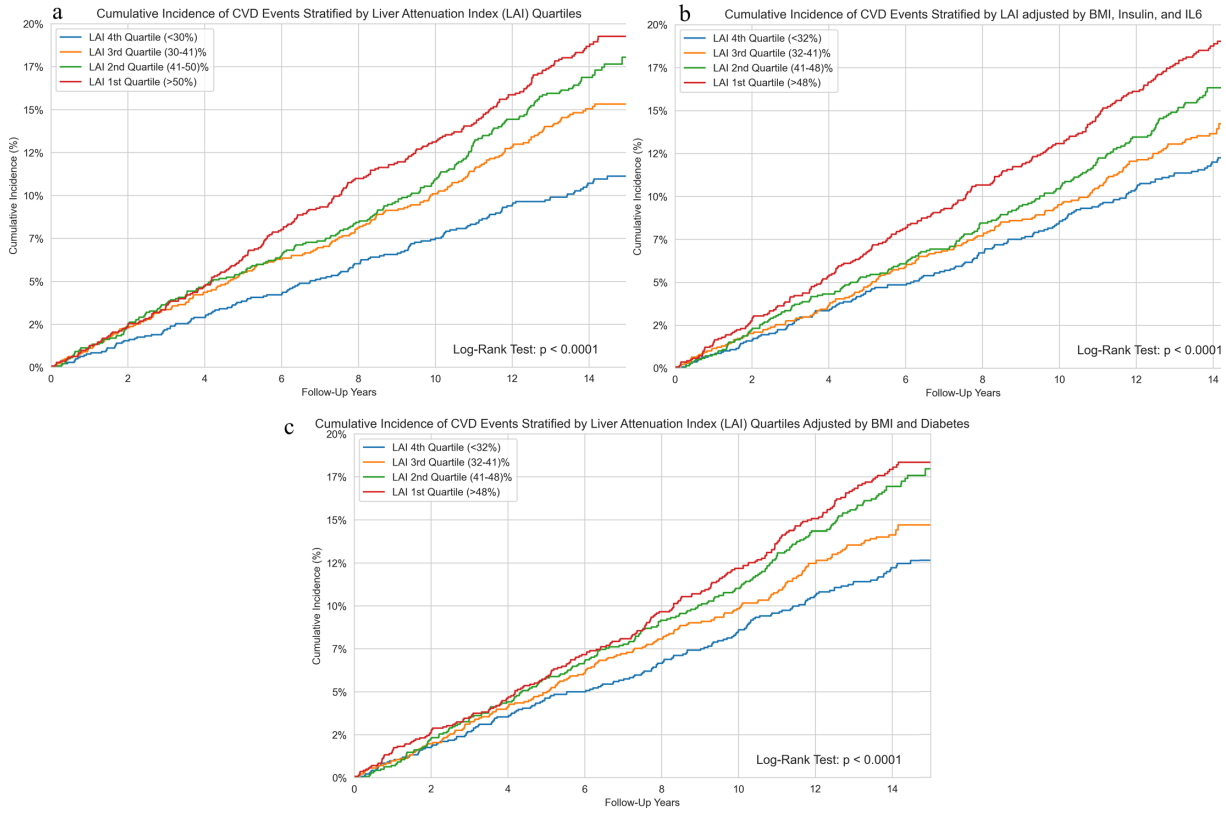

Figure 5 (a–c) 15-year cardiovascular disease (CVD) incidence by liver attenuation index (LAI), adjusted for body mass index (BMI), diabetes, interleukin (IL)-6, and insulin.

and all-cause mortality (HR 1.36, 95% CI 1.10 to 1.67) compared with those in the lowest quartile (Q1), independent of CVD risk factors and the Agatston CAC score. However, the association with CHD was not statistically significant (HR 1.29, 95% CI 0.91 to 1.83) (table 2).

In BMI-adjusted models, females in the highest quartile of LAI (Q4) compared with the lowest quartile (Q1) showed a higher risk of CVD (HR 1.42, 95% CI 0.93 to 2.16) and CHD (HR 1.20, 95% CI 0.66 to 2.17), although these associations were not statistically significant (table 2). The association between LAI Q4 and all-cause mortality showed significantly increased risk compared with Q1 (HR 1.51, 95% CI 1.12 to 2.03). Females in the third quartile (Q3) also exhibited a significantly

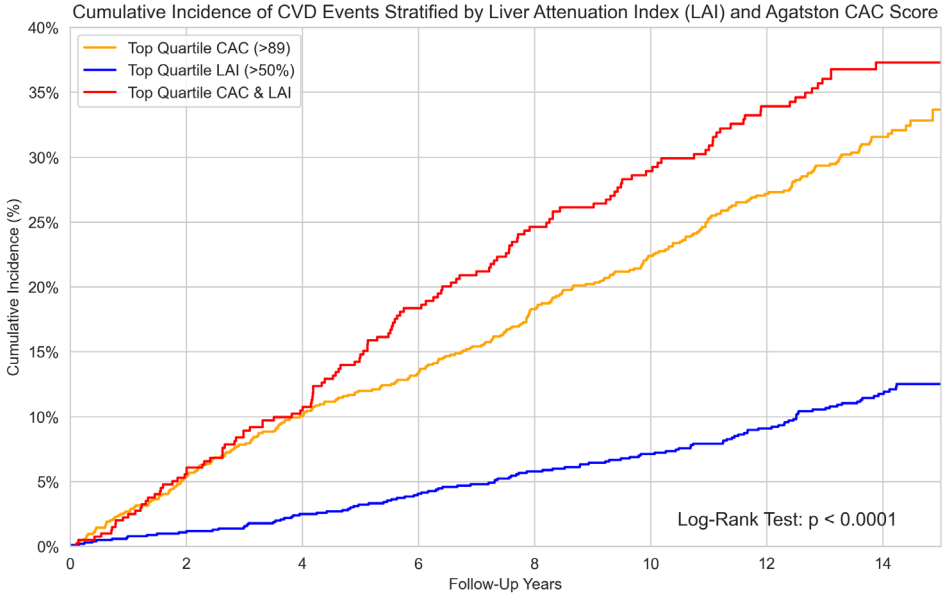

Figure 6 15-year cardiovascular disease (CVD) incidence by liver attenuation index (LAI) and Agatston coronary artery calcium (CAC) score.

Table 2 Minimally and fully adjusted HRs of incident CVD by the fourth quartile (Q4) vs first quartile (Q1) of LAI

	Overall: LAI Q4 vs Q1*	Male: LAI Q4 vs Q1†	Female: LAI Q4 vs Q1‡
BMI-adjusted HRs			
CVD	2.01 (1.54, 2.61)	1.54 (1.08, 2.2)	1.42 (0.93, 2.16)
CHD	1.96 (1.41, 2.71)	1.42 (0.94, 2.15)	1.2 (0.66, 2.17)
Stroke	2.07 (1.31, 3.27)	2.59 (1.37, 4.9)	1.28 (0.75, 2.21)
Mortality	1.69 (1.4, 2.05)	1.29 (0.99, 1.68)	1.51 (1.12, 2.03)
Fully adjusted HRs§			
CVD	1.43 (1.08, 1.89)	1.3 (0.91, 1.86)	1.18 (0.76, 1.82)
CHD	1.29 (0.91, 1.83)	1.22 (0.8, 1.86)	0.89 (0.48, 1.65)
Stroke	1.77 (1.09, 2.88)	2.05 (1.09, 3.86)	1.08 (0.62, 1.9)
Mortality	1.36 (1.1, 1.67)	1.07 (0.82, 1.41)	1.25 (0.92, 1.71)

*LAI quartiles: Q1 (<30%), Q2 (30.0%–41.0%), Q3 (41.1%–50.0%), Q4 (>50.0%).
†Male LAI quartiles: Q1 (<34.1%), Q2 (34.1%–43.5%), Q3 (43.6%–52.4%), Q4 (>52.4%).
‡Female LAI quartiles: Q1 (<27.0%), Q2 (27.0%–37.8%), Q3 (37.9%–47.5%), Q4 (>47.5%).
§Fully adjusted covariates: age, dyslipidemia, hypertension, smoking, diabetes, BMI, interleukin-6, insulin, C reactive protein, and Agatston CAC score.
BMI, body mass index; CAC, coronary artery calcium; CHD, coronary heart disease; CVD, cardiovascular disease; LAI, liver attenuation index.

elevated risk of mortality compared with Q1 (HR 1.44, 95% CI 1.12 to 1.86) (online supplemental table 1). After further adjustment by all CVD risk factors and Agatston CAC score, the risk of mortality remained elevated for women in LAI Q3 vs Q1 (HR 1.34, 95% CI 1.04 to 1.74). However, the association with CVD for females in Q4 vs Q1 remained insignificant (HR 1.18, 95% CI 0.76 to 1.82) along with Q3 vs Q1 and Q2 vs Q1.

In BMI-adjusted models, males in the highest quartile of LAI (Q4) had a significantly increased risk of CVD (HR 1.54, 95% CI 1.08 to 2.20) and stroke (HR 2.59, 95% CI 1.37 to 4.90) compared with Q1 (table 2). Elevated risk of mortality was observed (HR 1.29, 95% CI 0.99 to 1.68) but was not statistically significant, as the CI crossed 1. The third quartile (Q3) also showed elevated risks for CVD (HR 1.46, 95% CI 1.08 to 1.99), stroke (HR 2.11, 95% CI 1.21 to 3.67), and mortality (HR 1.41, 95% CI 1.12 to 1.78) (online supplemental table 2). In fully adjusted models, the highest quartile of LAI in males remained significantly associated with stroke risk (HR 2.05, 95% CI 1.09 to 3.86) compared with Q1 and Q3 showed a borderline significant stroke risk compared with Q1 (HR 1.76, 95% CI 1.00 to 3.09). The association with mortality was no longer significant (HR 1.07, 95% CI 0.82 to 1.41).

Analysis of continuous HRs

In males, each SD increase in LAI was associated with an HR of 1.14 (95% CI 1.01 to 1.28) for CVD events, independent of CVD risk factors plus Agatston CAC score. Each SD decrease of liver mean attenuation was associated with similar, but slightly lower risk (HR 0.89, 95% CI 0.78 to 1.0). For stroke events, the HR per SD increase of LAI was 1.31 (95% CI 1.04 to 1.66), independent of CVD risk factors plus Agatston CAC score. Each SD decrease in liver mean attenuation was not significant for stroke events (HR 0.81, 95% CI 0.64 to 1.02, p=0.16). In females, the HR per SD increase of LAI for mortality was 1.16 (95% CI 1.04 to 1.29) after adjustment for other CVD risk factors plus CAC score. Each SD decrease of liver mean attenuation was associated with similar risk (HR 0.83, 95% CI 0.72 to 0.95). No significant association with incident CVD was observed in females after adjustment for CVD risk factors plus Agatston CAC score.

Among non-Hispanic White individuals, each SD increase in LAI was significantly associated with CVD events (HR 1.17, 95% CI 1.0 to 1.36) independently of other CVD risk factors plus CAC score. In non-Hispanic Black individuals, a significant association was observed for overall mortality (HR 1.17, 95% CI 1.03 to 1.33); similarly, in Hispanic individuals, LAI was significantly associated with higher overall mortality (HR 1.23, 95% CI 1.04 to 1.46). No significant associations were found in the Chinese subgroup independent of CVD risk factors plus CAC score.

DISCUSSION

To our knowledge, this is the first AI-generated opportunistic CT quantification of liver steatosis in CAC scans that analyzed the entire liver within the field of view. We found that the LAI is a predictor of CVD events and all-cause mortality independent of traditional risk factors. Notably, the association with CVD events and all-cause mortality remained when adjusting for CAC score. The LAI approach led to slightly improved discrimination for CVD events compared with using the liver mean HU. When analyzing the time-dependent receiver operating characteristic (ROC) curve and the area under the curve (AUC) for LAI+CVD risk factors compared with CVD risk factors alone, we did not observe a significant difference.

However, we found people in the highest quartile of both LAI and CAC score experienced a higher incidence of CVD events compared with those in the highest quartile of CAC score or LAI alone. Our AI-enabled approach differs from previously reported methods in which liver attenuation was measured in small regions of interest.[7 9 12 26–28] Our approach may provide more robust measurements because it allows the heterogeneity of fat deposition throughout the liver to be captured. Furthermore, we demonstrated correlations between LAI and known cardiometabolic risk factors such as obesity, dyslipidemia, and diabetes.

Our findings are in line with prior studies in MESA and other cohorts using a manual method of measuring NAFLD defined by a liver-to-spleen ratio below 1.0. In these manual methods, the measurements were done in approximately 1 cm radii in the anterior and posterior lobes of liver, and one sample in the spleen. These studies found NAFLD was associated with incident non-fatal CHD and all-cause mortality after adjusting for traditional risk factors.[29–31] We found LAI varied significantly by race/ethnicity and was the highest in Hispanic subjects, consistent with a previous study in MESA in which Hispanic subjects experienced the highest proportion of NAFLD classified using the liver-to-spleen ratio.[32] Despite adjustments for known CVD risk factors, we are unable to conclude whether increased CVD and all-cause mortality risks are directly linked to high LAI or mediated by diabetes, which is linked to liver steatosis. The pathogenesis linking steatosis with type 2 diabetes is complex, and accumulating evidence now indicates the two are strongly related.[33] Liver steatosis, reflected in an elevated LAI score, is a strong predictor of incident type 2 diabetes, which in turn leads to excess CVD and mortality, as reported by investigators in other cohorts.[34–36] The strong relationship between liver steatosis and development of type 2 diabetes has also been validated in previous studies in MESA using manually measured liver attenuation in chest CT.[37–39] A recent meta-analysis of 2877 participants undergoing CCT found that the presence of hepatic steatosis was associated with a twofold increase in risk of high-risk coronary plaque.[40] It is noteworthy that as photon-counting multispectral CT scanners become increasingly available, the accuracy of CT quantification of fatty liver may rival that of MRI.[41 42]

Early disease detection is a prerequisite for primary prevention. CAC screening, with opportunistic extraction of actionable information (using existing guidelines and care pathways), is a promising approach for early detection of multiple conditions including CHD, heart failure, atrial fibrillation, stroke, osteoporosis, steatosis, and other abnormalities that often interplay and contribute to poor outcomes.[15–18 20 43 44] Additionally, the same technique can be applied to both abdominal and non-gated lung cancer screening scans, potentially reaching a larger population who may not be actively seeking CVD risk assessment. Our approach can best serve primary care doctors because MRI and ultrasound imaging of liver fat are unavailable for primary care settings and cannot be performed as an add-on opportunistically. In contrast, our AI software is readily accessible in such settings, providing a significant advantage from a public health perspective.

For example, the AI software can function as an opportunistic screening tool within the background of radiology picture archiving and communication system, flagging high-risk individuals for follow-up, many of whom might not have previously undergone cardiovascular risk factor assessment.

Others have reported similar opportunistic measurements in CT scans.[45] With the expansion of AI-enabled early detection, it is imperative for professional societies from diverse disciplines—such as cardiology, pulmonology, endocrinology, gastroenterology/hepatology and lung cancer—to collaborate in developing guidelines for implementing opportunistic disease assessments to improve patient care. In this context, one can anticipate future 'incidental' findings to become 'intentional' findings.

In this study, after adjustment for BMI, Black individuals had the lowest LAI, while Hispanic individuals had the highest LAI. However, we have observed a higher risk of all-cause mortality in both Black and Hispanic individuals with higher LAI. While we acknowledge that certain AI algorithms may enforce unwanted and unconscious biases that perpetuate existing healthcare disparities, particularly related to race and ethnicity, we do not anticipate such biases in our results. The reason is that the AI-CVD liver segmentation only identifies the liver and reports the percentage of liver voxels with HU <40. There is no AI interpretation regarding sex or race/ethnicity in this process. Furthermore, as the largest multi-ethnic study of CVD risk factors, MESA recruited a diverse population from six US communities, representing various races and ethnicities (Baltimore, Maryland; Chicago, Illinois; Forsyth County, North Carolina; Los Angeles County, California; Northern Manhattan, New York; and St. Paul, Minnesota), which included non-Hispanic White (38%), non-Hispanic Black (28%), Chinese (11%), and Hispanic (11%) individuals.

Limitations

A potential limitation of the approach used for liver quantification in this study is that the volume analyzed may include vessels and other structures that are not part of the liver parenchyma. Additionally, this technique may be more sensitive to image noise and thus its usefulness in low-dose CT scans needs to be further evaluated; however, we adjusted voxel thresholds to the (−30, 70) HU range and adjusted for BMI to minimize the impact of noise in this study.

Another limitation of our study is that MESA does not have information on how many participants had NAFLD/ALD at baseline. While reported current alcohol use did not differ significantly between quartiles of LAI, those in the lowest quartile of LAI (<32%) reported 50% fewer

drinks per week compared with others (1 (0–5) drink per week vs 2 (0–6)).

CONCLUSION

Analysis of LAI based on the entire liver visible in CAC scans provides opportunistic and actionable information for early detection of patients at elevated risk of CVD events and all-cause mortality. The clinical utility of incorporating LAI along with other opportunistic findings in CAC scans as part of the AI-CVD initiative to improve CVD risk prediction warrants investigation in other cohorts.

Author affiliations
[1]HeartLung Technologies, Houston, Texas, USA
[2]Cornell University, Ithaca, California, USA
[3]University of Basel, Basel, Switzerland
[4]Tustin Teleradiology, Tustin, California, USA
[5]Mount Sinai Medical Center, New York, New York, USA
[6]The Lundquist Institute, Torrance, California, USA
[7]Icahn School of Medicine at Mount Sinai, New York, New York, USA
[8]University of California, Irvine, California, USA
[9]Houston Methodist, Houston, Texas, USA
[10]Stanford University School of Medicine, Stanford, California, USA
[11]University of Houston, Houston, Texas, USA
[12]The University of Texas Health Science Center at Houston, Houston, Texas, USA
[13]University of Louisville, Louisville, Kentucky, USA
[14]Cedars-Sinai Medical Center, Los Angeles, California, USA
[15]Michigan State University, East Lansing, Michigan, USA
[16]University of Groningen, Groningen, The Netherlands
[17]National Institutes of Health, Bethesda, Maryland, USA

Acknowledgements The authors thank the other investigators, the staff, and the participants of the MESA study for their valuable contributions. A full list of participating MESA investigators and institutions can be found at http://www.mesa-nhlbi.org.

Contributors MN is the guarantor for this work and accepts full responsibility for the integrity and accuracy of the manuscript. All authors have read and approved the manuscript for submission. MN: conceptualization of the study, research design, proposal to MESA, project administration, writing the original draft, and revision and editing. KA: data analysis, figure design, data interpretation, AI development, manuscript writing, revision, and editing. AR, CZ, JW: AI development and interpretation. TA, CH, DY: research design, manuscript brainstorming, reviewing data analysis, revisions, and editing. JJZ: reviewing manuscript content. MJB: proposal to MESA, manuscript brainstorming, reviewing data analysis, revisions, and editing. ADB: manuscript brainstorming, reviewing data analysis, revisions, and editing. NM, WF, SKR, KN, SM, ZF, MVMcC, RY, IK, DJM, JN, KW, PKS, GA, RV and DL: manuscript brainstorming, reviewing data analysis, revisions, and editing. NDW: project administration, overseeing research, research design, proposal to MESA, manuscript brainstorming, reviewing data analysis, critical revisions and editing.

Funding This research was supported by U01OH012622, U01CA288425, 2R42AR070713, and R01HL146666. Baseline liver analysis in MESA was supported by R01 HL071739. MESA was supported by contracts 75N92020D00001, HHSN268201500003I, N01-HC-95159, 75N92020D00005, N01-HC-95160, 75N92020D00002, N01-HC-95161, 75N92020D00003, N01-HC-95162, 75N92020D00006, N01-HC-95163, 75N92020D00004, N01-HC-95164, 75N92020D00007, N01-HC-95165, N01-HC-95166, N01-HC-95167, N01-HC-95168, and N01-HC-95169 from the National Heart, Lung, and Blood Institute, and by grants UL1-TR-000040, UL1-TR-001079, and UL1-TR-001420 from the National Center for Advancing Translational Sciences (NCATS).

Disclaimer The views expressed in this manuscript are those of the authors and do not necessarily represent the views of the National Heart, Lung, and Blood Institute; the National Institutes of Health; or the US Department of Health and Human Services.

Competing interests MN is the founder of HeartLung Technologies, which is the developer of the AI software used in this study. AR, TA, DY, and NDW are advisors to HeartLung Technologies. JJZ is an advisor to HeartLung Technologies and Median Technologies, and co-founder of Oncoswab. CZ is a software engineer and employee of HeartLung Technologies. KA is a data scientist and research associate of HeartLung Technologies. MVMcC is Chief Health Officer at Toku. The remaining authors declare no competing interests

Patient consent for publication Not applicable.

Ethics approval As a longitudinal population-based study sponsored by the National Institutes of Health (NIH), MESA has received proper ethical oversight. The MESA protocol was approved by the Institutional Review Board (IRB) of the six field medical centers (Columbia University IRB#9246, Johns Hopkins Medicine, Northwestern University, University of California, Los Angeles, University of Minnesota, Wake Forest) and the National Heart, Lung, and Blood Institute. Data from participants who did not consent to commercial use were removed from our study.

Provenance and peer review Not commissioned; externally peer reviewed.

Data availability statement Data are available on reasonable request. The demographic data and outcomes from MESA Exam 1 used in this study are available from the Multi-Ethnic Study of Atherosclerosis (MESA). Data access is subject to approval and adherence to the MESA Data Distribution Agreement. Researchers interested in accessing the MESA Exam 1 data can submit a request through the MESA website (MESA Data Access) and follow the guidelines provided for data use. For additional information on data access and usage policies, please visit the MESA official website or contact the MESA Coordinating Center at MESA Contact Information.

ORCID iD
Morteza Naghavi http://orcid.org/0000-0001-8112-175X

REFERENCES

1 Ilagan-Ying YC, Banini BA, Do A, *et al*. Screening, Diagnosis, and Staging of Non-Alcoholic Fatty Liver Disease (NAFLD): Application of Society Guidelines to Clinical Practice. *Curr Gastroenterol Rep* 2023;25:213–24.
2 Lee ECZ, Anand VV, Razavi AC, *et al*. The Global Epidemic of Metabolic Fatty Liver Disease. *Curr Cardiol Rep* 2024;26:199–210.
3 Ha Y, Jeong I, Kim TH. Alcohol-Related Liver Disease: An Overview on Pathophysiology, Diagnosis and Therapeutic Perspectives. *Biomedicines* 2022;10:2530.
4 Moon JH, Jeong S, Jang H, *et al*. Metabolic dysfunction-associated steatotic liver disease increases the risk of incident cardiovascular disease: a nationwide cohort study. *EClinicalMedicine* 2023;65:102292.
5 Del Villar-Carrero RS, Blanco A, Ruiz LD, *et al*. Bridging Metabolic-Associated Steatotic Liver Disease and Cardiovascular Risk: A Potential Role for Ketogenesis. *Biomedicines* 2024;12:692.
6 Ndumele CE, Rangaswami J, Chow SL, *et al*. Cardiovascular-Kidney-Metabolic Health: A Presidential Advisory From the American Heart Association. *Circulation* 2023;148:1606–35.
7 Starekova J, Hernando D, Pickhardt PJ, *et al*. Quantification of Liver Fat Content with CT and MRI: State of the Art. *Radiology* 2021;301:250–62.
8 Harvard Health. Radiation risk from medical imaging. 2010. Available: https://www.health.harvard.edu/cancer/radiation-risk-from-medical-imaging [Accessed 08 Oct 2024].
9 Pickhardt PJ, Jee Y, O'Connor SD, *et al*. Visceral adiposity and hepatic steatosis at abdominal CT: association with the metabolic syndrome. *AJR Am J Roentgenol* 2012;198:1100–7.

10 Park SH, Kim PN, Kim KW, *et al*. Macrovesicular Hepatic Steatosis in Living Liver Donors: Use of CT for Quantitative and Qualitative Assessment. *Radiology* 2006;239:105–12.
11 Kodama Y, Ng CS, Wu TT, *et al*. Comparison of CT methods for determining the fat content of the liver. *AJR Am J Roentgenol* 2007;188:1307–12.
12 Ma X, Holalkere N-S, Kambadakone R A, *et al*. Imaging-based quantification of hepatic fat: methods and clinical applications. *Radiographics* 2009;29:1253–77.
13 Haghshomar M, Antonacci D, Smith AD, *et al*. Diagnostic Accuracy of CT for the Detection of Hepatic Steatosis: A Systematic Review and Meta-Analysis. *Radiology* 2024;313:e241171.
14 Naghavi M, Reeves A, Atlas K, *et al*. Abstract 4144083: AI-CVD: Artificial Intelligence-Enabled Opportunistic Screening of Coronary Artery Calcium Computed Tomography Scans for Predicting CVD Events and All-Cause Mortality: The Multi-Ethnic Study of Atherosclerosis (MESA). *Circulation* 2024;150.
15 Naghavi M, Atlas K, Jaberzadeh A, *et al*. Validation of Opportunistic Artificial Intelligence-Based Bone Mineral Density Measurements in Coronary Artery Calcium Scans. *J Am Coll Radiol* 2024;21:624–32.
16 Naghavi M, De Oliveira I, Mao SS, *et al*. Opportunistic AI-enabled automated bone mineral density measurements in lung cancer screening and coronary calcium scoring CT scans are equivalent. *Eur J Radiol Open* 2023;10:100492.
17 Naghavi M, Yankelevitz D, Reeves AP, *et al*. AI-enabled left atrial volumetry in coronary artery calcium scans (AI-CAC™) predicts atrial fibrillation as early as one year, improves CHARGE-AF, and outperforms NT-proBNP: The multi-ethnic study of atherosclerosis. *J Cardiovasc Comput Tomogr* 2024;18:383–91.
18 Naghavi M, Reeves A, Budoff M, *et al*. AI-enabled cardiac chambers volumetry in coronary artery calcium scans (AI-CAC™) predicts heart failure and outperforms NT-proBNP: The multi-ethnic study of Atherosclerosis. *J Cardiovasc Comput Tomogr* 2024;18:392–400.
19 Naghavi M, Reeves AP, Atlas KC, *et al*. AI-Enabled CT Cardiac Chamber Volumetry Predicts Atrial Fibrillation and Stroke Comparable to MRI. *JACC Adv* 2024;3:101300.
20 Naghavi M, Reeves A, Atlas K, *et al*. AI-enabled cardiac chambers volumetry and calcified plaque characterization in coronary artery calcium (cac) scans (ai-cac) significantly improves on agatston cac score for predicting all cardiovascular events: the multi-ethnic study of atherosclerosis. *Res Sq* [Preprint] 2024.
21 Bild DE, Bluemke DA, Burke GL, *et al*. Multi-Ethnic Study of Atherosclerosis: objectives and design. *Am J Epidemiol* 2002;156:871–81.
22 Wasserthal J, Meyer M, Breit HC, *et al*. TotalSegmentator: robust segmentation of 104 anatomical structures in CT images. *arXiv* 2022.
23 Wasserthal J. Wasserth/totalsegmentator. 2024. Available: https://github.com/wasserth/TotalSegmentator [Accessed 15 Apr 2024].
24 Carr JJ, Nelson JC, Wong ND, *et al*. Calcified coronary artery plaque measurement with cardiac CT in population-based studies: standardized protocol of Multi-Ethnic Study of Atherosclerosis (MESA) and Coronary Artery Risk Development in Young Adults (CARDIA) study. *Radiology* 2005;234:35–43.
25 Ruhl CE, Everhart JE. Fatty liver indices in the multiethnic United States National Health and Nutrition Examination Survey. *Aliment Pharmacol Ther* 2015;41:65–76.
26 McAuley PA, Hsu F-C, Loman KK, *et al*. Liver attenuation, pericardial adipose tissue, obesity, and insulin resistance: the Multi-Ethnic Study of Atherosclerosis (MESA). *Obesity (Silver Spring)* 2011;19:1855–60.
27 Al Rifai M, Silverman MG, Nasir K, *et al*. The association of nonalcoholic fatty liver disease, obesity, and metabolic syndrome, with systemic inflammation and subclinical atherosclerosis: the Multi-Ethnic Study of Atherosclerosis (MESA). *Atherosclerosis* 2015;239:629–33.
28 Pickhardt PJ, Graffy PM, Reeder SB, *et al*. Quantification of Liver Fat Content With Unenhanced MDCT: Phantom and Clinical Correlation With MRI Proton Density Fat Fraction. *AJR Am J Roentgenol* 2018;211:W151–7.
29 Zeb I, Li D, Nasir K, *et al*. Computed tomography scans in the evaluation of fatty liver disease in a population based study: the multi-ethnic study of atherosclerosis. *Acad Radiol* 2012;19:811–8.
30 Zeb I, Li D, Budoff MJ, *et al*. Nonalcoholic Fatty Liver Disease and Incident Cardiac Events: The Multi-Ethnic Study of Atherosclerosis. *J Am Coll Cardiol* 2016;67:1965–6.
31 Ahmed HS, Wang N, Carr JJ, *et al*. The association between hepatic steatosis and incident cardiovascular disease, cancer, and all-cause mortality in a US multicohort study. *Hepatology* 2023;77:2063–72.
32 Tota-Maharaj R, Blaha MJ, Zeb I, *et al*. Ethnic and sex differences in fatty liver on cardiac computed tomography: the multi-ethnic study of atherosclerosis. *Mayo Clin Proc* 2014;89:493–503.
33 Xiong X, Li X. Type 2 diabetes originated from non-alcoholic fatty liver disease. *Life Metab* 2023;2:load007.
34 Mantovani A, Byrne CD, Bonora E, *et al*. Nonalcoholic Fatty Liver Disease and Risk of Incident Type 2 Diabetes: A Meta-analysis. *Diabetes Care* 2018;41:372–82.
35 Lonardo A, Ballestri S, Guaraldi G, *et al*. Fatty liver is associated with an increased risk of diabetes and cardiovascular disease - Evidence from three different disease models: NAFLD, HCV and HIV. *World J Gastroenterol* 2016;22:9674–93.
36 Oni ET, Agatston AS, Blaha MJ, *et al*. A systematic review: burden and severity of subclinical cardiovascular disease among those with nonalcoholic fatty liver; should we care? *Atherosclerosis* 2013;230:258–67.
37 Oni E, Ogunmoroti O, Allen N, *et al*. Life's Simple 7 and Nonalcoholic Fatty Liver Disease: The Multiethnic Study of Atherosclerosis. *Am J Med* 2021;134:519–25.
38 Rodriguez LA, Kanaya AM, Shiboski SC, *et al*. Does NAFLD mediate the relationship between obesity and type 2 diabetes risk? evidence from the multi-ethnic study of atherosclerosis (MESA). *Ann Epidemiol* 2021;63:15–21.
39 Shah RV, Allison MA, Lima JAC, *et al*. Liver fat, statin use, and incident diabetes: The Multi-Ethnic Study of Atherosclerosis. *Atherosclerosis* 2015;242:211–7.
40 Sukudom S, Wee J, Huangfu G, *et al*. Hepatic Steatosis and High-Risk Coronary Plaque: A Systematic Review. *JACC Cardiovasc Imaging* 2024;17:1392–4.
41 Schwartz FR, Ashton J, Wildman-Tobriner B, *et al*. Liver fat quantification in photon counting CT in head to head comparison with clinical MRI - First experience. *Eur J Radiol* 2023;161:110734.
42 Lin H, Xu X, Deng R, *et al*. Photon-counting Detector CT for Liver Fat Quantification: Validation across Protocols in Metabolic Dysfunction-associated Steatotic Liver Disease. *Radiology* 2024;312:e240038.
43 Naghavi M, Reeves AP, Atlas K, *et al*. Coronary artery calcium scans powered by artificial intelligence predicts atrial fibrillation comparably to cardiac magnetic resonance imaging: the multi-ethnic study of atherosclerosis (MESA). *Radiology and Imaging* [Preprint] 2024.
44 Naghavi M, Reeves A, Atlas K, *et al*. Abstract 4144043: Automated Left Ventricular Volumetry using Artificial Intelligence in Coronary Calcium Scans (AI-CAC) Predicts Heart Failure Comparably to Cardiac MRI and Outperforms NT-proBNP: The Multi-Ethnic Study of Atherosclerosis (MESA). *Circulation* 2024;150.
45 Pickhardt PJ, Graffy PM, Zea R, *et al*. Automated CT biomarkers for opportunistic prediction of future cardiovascular events and mortality in an asymptomatic screening population: a retrospective cohort study. *Lancet Digit Health* 2020;2:e192–200.